

## Gene expression profiling of potential PPAR $\gamma$ target genes in mouse aorta

Henry L. Keen,<sup>1,2</sup> Michael J. Ryan,<sup>1</sup> Andreas Beyer,<sup>1</sup> Satya Mathur,<sup>1</sup> Todd E. Scheetz,<sup>2</sup> Barry D. Gackle,<sup>2</sup> Frank M. Faraci,<sup>1</sup> Thomas L. Casavant,<sup>2</sup> and Curt D. Sigmund<sup>1</sup>

<sup>1</sup>Departments of Internal Medicine and Physiology and Biophysics, and the <sup>2</sup>Center for Bioinformatics and Computational Biology, University of Iowa College of Medicine, Iowa City, Iowa 52242

Submitted 9 February 2004; accepted in final form 25 March 2004

**Keen, Henry L., Michael J. Ryan, Andreas Beyer, Satya Mathur, Todd E. Scheetz, Barry D. Gackle, Frank M. Faraci, Thomas L. Casavant, and Curt D. Sigmund.** Gene expression profiling of potential PPAR $\gamma$  target genes in mouse aorta. *Physiol Genomics* 18: 33–42, 2004. First published March 30, 2004; 10.1152/physiolgenomics.00027.2004.—Diminished activity of peroxisome proliferator-activated receptor- $\gamma$  (PPAR $\gamma$ ) may play a role in the pathogenesis of hypertension and vascular dysfunction. To better understand what genes are regulated by PPAR $\gamma$ , an experimental data set was generated by microarray analysis, in duplicate, of pooled aortic mRNA isolated from mice treated for 21 days with a PPAR $\gamma$  agonist (rosiglitazone) or vehicle. Of the 12,488 probe sets present on the array (Affymetrix MG-U74Av2), 181 were differentially expressed between groups according to a statistical metric generated using Affymetrix software. A significant correlation was observed between the microarray results and real-time RT-PCR analysis of 39 of these genes. Cluster analysis revealed 3 expression patterns, 29 transcripts of moderate abundance that were decreased (–93%) to very low levels, 106 transcripts that were downregulated (–42%), and 46 transcripts that were upregulated (+70%). Functional groups that were decreased included inflammatory response (–93%,  $n = 6$ ), immune response (–86%,  $n = 7$ ), and cytokines (–82%,  $n = 7$ ). There was an overall upregulation in the oxidoreductase activity group (+47%,  $n = 9$ ). Individually, six transcripts in this group were increased (+72%), and three were decreased (–34%). Fourteen of the genes map to regions in the rat genome that have been linked to increased blood pressure, and of 142 upstream regions analyzed, sequences resembling the DNA binding site for PPAR $\gamma$  were identified in 101 of the differentially expressed genes.

gene expression analysis; bioinformatics; vasculature; mouse; transcription factor

THE PEROXISOME PROLIFERATOR-ACTIVATED receptor- $\gamma$  (PPAR $\gamma$ ) is a member of the nuclear hormone receptor subfamily of transcription factors and acts by forming heterodimers with retinoid X receptors. Ligands that activate PPAR $\gamma$  include a naturally occurring prostaglandin J metabolite [15d-PGJ(2)] and a group of synthetic compounds, thiazolidinediones (TZDs). Several lines of evidence demonstrate an important role for PPAR $\gamma$  in lipid and glucose metabolism. PPAR $\gamma$  is highly expressed in adipose tissue and induces adipocyte differentiation (20). Chronic administration of TZDs in humans with type II diabetes decreases release of free fatty acids (FFA) from adipose tissue (17) and significantly improves insulin sensitivity (18). In addition to these well-characterized metabolic

actions of PPAR $\gamma$ , recent experimental evidence suggests involvement in a number of other pathways including cell-cycle regulation, inflammation, and vascular function (3).

It has recently been demonstrated that PPAR $\gamma$  is expressed in all cell types [vascular smooth muscle cells (13), endothelial cells (5), and macrophages (22)] in the vasculature, and current evidence suggests that PPAR $\gamma$  may normally mediate an important vascular protective action. Pharmacological activation of PPAR $\gamma$  with TZDs reduces vascular lesion formation in animal models of atherosclerosis (4) and inhibits vascular smooth muscle cell proliferation and neointima formation after balloon injury (14). Chronic reduction in blood pressure and improvement in endothelial function has been observed during TZD administration in humans and animal models (21, 27, 29). Moreover, naturally occurring loss-of-function mutations in human PPAR $\gamma$  are associated with hypertension (2).

We and others hypothesize that PPAR $\gamma$  plays an important role in vascular function and hypertension. Although many targets for PPAR $\gamma$  have been identified in skeletal muscle and fat, the classic PPAR $\gamma$  target organs, little is known about the genes or gene networks that are directly regulated by this factor in the vasculature. Because PPAR $\gamma$  is a transcription factor, its physiological actions depend on binding to a specific DNA sequence, recruiting cofactors, and then activating/repressing transcription of target genes. Given the availability of genomic sequence, some investigators have employed a strategy of searching for transcription factor binding sites as a means to identify potential new downstream targets of various transcription factors (10, 25). In the present study, we have combined this and other types of computational approaches with large-scale gene expression analysis using microarrays to identify potential downstream targets of PPAR $\gamma$  and to generate hypotheses regarding the biological function and transcriptional regulation of PPAR $\gamma$  regulated genes in the vascular wall.

### METHODS

The microarray data described in the present study complies with the MIAME (“minimum information about microarray experiment”) standard, has been deposited in the National Center for Biotechnology Information (NCBI) Gene Expression Omnibus (GEO) database, and can be accessed at <http://www.ncbi.nlm.nih.gov/geo> (accession number: GSE1011).

**Animal care.** All procedures and care of the mice were conducted in accordance with National Institutes of Health guidelines using protocols approved by the Animal Care and Use Committee of the University of Iowa. Mice were fed standard mouse chow and received water ad libitum.

**Experimental protocols.** To activate PPAR $\gamma$ , the TZD rosiglitazone was administered for 21 days by oral gavage to adult male mice (C57BL/6J strain) at a dose of 25 mg·kg<sup>–1</sup>·day<sup>–1</sup>. Control mice were given vehicle (sterile water). This dose is similar to that which has been reported in the literature for animal studies but is higher than the

Article published online before print. See web site for date of publication (<http://physiolgenomics.physiology.org>).

Address for reprint requests and other correspondence: C. D. Sigmund, Depts. of Internal Medicine and Physiology and Biophysics, 3181B Medical Education and Biomedical Research Facility, Roy J. and Lucille A. Carver College of Medicine, Univ. of Iowa, Iowa City, IA 52242 (E-mail: [curt-sigmund@uiowa.edu](mailto:curt-sigmund@uiowa.edu)).

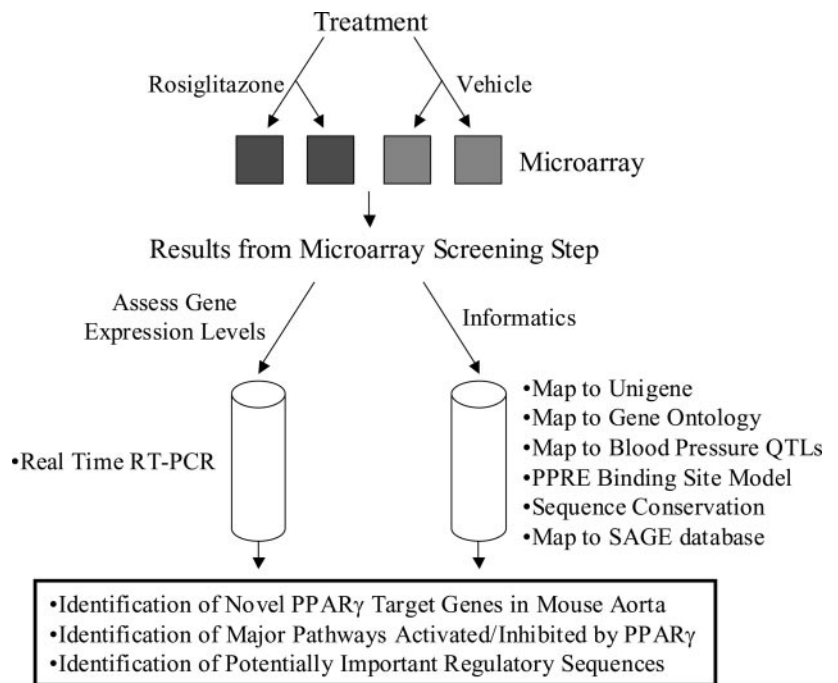


Fig. 1. Basic schema of the experimental and informatics methods used in the present study to examine the peroxisome proliferator-activated receptor- $\gamma$  (PPAR $\gamma$ ) pathway in mouse aorta.

standard dose reported for the treatment of non-insulin-dependent diabetes mellitus. At the end of the experiment, mice were killed by CO<sub>2</sub> asphyxiation, and the aorta was immediately immersed in RNA-later solution (Qiagen). Total RNA was isolated from aortic samples using a commercially available RNeasy Miniprep kit (Qiagen). The quality of the RNA was confirmed by visual inspection of the 18S and 28S ribosomal RNA bands on an ethidium bromide-stained 1.5% agarose gel. To have sufficient RNA for both the microarray hybridizations (in duplicate) and the real-time RT-PCR analysis, RNA from 4–5 mice in each group were pooled.

**Microarray analysis.** Because the amount of starting RNA for each array experiment was low (less than 1  $\mu$ g), two rounds of linear amplification were performed to produce sufficient material for hybridization to the array. The hybridization, washing steps, and scanning of the array were performed in the University of Iowa Microarray Facility using standard protocols. The relative amount of transcript was determined by comparing the perfect match and mismatch signals from all probe pairs. This signal value is a weighted mean value, relatively insensitive to outlier values, calculated using the one-step Tukey's biweight estimate. Determination of whether the difference in transcript intensity between two arrays was statistically significant was accomplished by using the Wilcoxon signed rank test. Only transcripts that were different in all between-group (i.e., vehicle vs. rosiglitazone) comparisons and that were not changed in all within-group comparisons (i.e., replicates) were considered to be differentially expressed. The Affymetrix microarray analysis suite was used to perform all of the above statistical tests.

**Sequence analysis.** Genomic DNA sequences (5 kb) immediately upstream of the transcriptional start site from known and predicted transcripts from mouse (22,444) and human (24,847) were downloaded from Ensembl (<http://www.ensembl.org>) using the EnsMart tool (12). Additional gene information including chromosomal location and human/mouse orthology was obtained from the same site. Processing of these data files was accomplished using custom Perl scripts. PPAR $\gamma$  has been shown to have important actions on blood pressure and vascular function. It is possible that some of the PPAR $\gamma$  target genes identified herein play a causal role in genetic hypertension. Therefore, to identify these potential candidate genes, we determined whether any of the differentially expressed genes are located

within known rat blood pressure quantitative trait loci (QTL) regions. This was accomplished by interspecies comparisons using syntenic maps from the Jackson Laboratory (<http://www.jax.org>) and from the Rat Genome Database (<http://rgd.mcw.edu>). To search for sequences closely resembling the PPAR response element (PPRE), we created a probabilistic-based model (hidden Markov model) based on the sequences of 19 known PPREs (Supplemental Table S1, available at the *Physiological Genomics* web site).<sup>1</sup> The software used to build the model is part of a freely available package (HMMER 2, Eddy, S.R., <http://hmmerr.wustl.edu/>). Noncoding sequences that are highly conserved between orthologous genomic sequences from different species are likely to contain important regulatory elements. To prioritize our list of potential PPREs, evolutionarily conserved sequences were identified by pairwise alignment of upstream sequences using a locally installed version of MegaBlast (<http://www.ncbi.nlm.nih.gov/blast>). Sequence fragments with 80% identity over at least 100 bp were considered to be highly conserved. Percent identity plots graphically depicting sequence conservation were downloaded from the Penn State University Center for Comparative Genomics and Bioinformatics (<http://bio.cse.psu.edu/>).

**Real-time RT-PCR analysis.** To validate the gene expression changes observed in the microarray experiment, expression of 39 genes was determined using a real-time quantitative PCR system (iCycler iQ multi-color real-time PCR detection system, Bio-Rad). These 39 genes were selected based on several criteria: 1) a representative mix of genes that included both up- and downregulated transcripts, 2) genes with known relevance to vascular physiology, and 3) genes with predicted PPREs in the regions upstream of the genes. Real-time reactions employed sequence-specific probes designed using commercial software (Applied Biosystems, Foster City, CA). Input samples were the same pooled RNA used in the microarray analysis.

**Other analysis.** Functional categories were generated by assigning each transcript a function based on the Gene Ontology ([<sup>1</sup>The Supplementary Material for this article \(Supplemental Tables S1–S4 and Supplemental Figs. S1 and S2\) is available online at <http://physiolgenomics.physiology.org/cgi/content/full/00027.2004/DC1>.](http://</a></p>
</div>
<div data-bbox=)

geneontology.org) database. We further examined the patterns of gene expression changes with cluster analysis using hierarchical clustering followed by more detailed grouping using the k-means algorithm. The software used is available for download free of charge to academic users (Cluster and TreeView, M. Eisen; <http://rana.lbl.gov/EisenSoftware.htm>).

**Statistical analysis.** Correlation analysis was performed by calculating the Pearson correlation coefficient using commercially available software (SigmaStat). *P* values less than 0.05 represent statistical significance.

## RESULTS

To examine the PPAR $\gamma$  pathway in mouse aorta, we followed the steps outlined in Fig. 1. Gene expression profiling with microarrays was used as a large-scale screening step to determine in a nonbiased manner what pathways are activated/inhibited by rosiglitazone and to generate a list of potential PPAR $\gamma$  target genes. Subsequently, quantitative real-time RT-PCR was used to determine the expression changes in 39 individual genes, and computational methods were used to identify potentially important regulatory sequences.

As a measure of the quality of the microarray experiment, the signal intensities of transcripts from each array were plotted as a histogram (Supplemental Fig. S1). They correctly approx-

imated a normal distribution with an expected modest skewing toward lower abundance transcripts. Under baseline conditions (vehicle-treated mice), 3,034 transcripts on the array (12,488 total) were expressed in both replicates. The expression levels of most transcripts were similar between replicates, demonstrating the reproducibility of the microarray assay (Supplemental Fig. S2). We also noticed that when we mapped the accession number associated with each probe set to the UniGene data set, that many genes were represented more than once on the microarray. For example, among genes that were expressed in all samples, 105 UniGenes were represented exactly 2 times on each array, and there was a statistically significant correlation ( $R^2 = 0.68$ ,  $P < 0.05$ ) between the fold change values (rosiglitazone vs. vehicle) calculated from these two probe sets (data not shown).

Using the criteria outlined in the METHODS, we identified 181 transcripts that were differentially expressed during chronic treatment with rosiglitazone (Supplemental Tables S2 and S3). To validate the microarray results, we performed real-time RT-PCR (using the same input RNA) on 39 of the differentially expressed genes (Table 1). There was a statistically significant correlation between these two different assays with an agreement of about 90% on the up/downregulated calls (Fig.

Table 1. Correlation between microarray and real-time RT-PCR

| Probe Set   | Accession No. | Description   | Array | RT-PCR |
|-------------|---------------|---|-------|--------|
| 93100_at    | X13297        | Actin, alpha 2, smooth muscle, aorta                        | 0.45  | 0.51   |
| 96573_at    | M21495        | Actin, gamma, cytoplasmic                                   | 0.55  | 0.89   |
| 161359_s_at | AV212934      | Apolipoprotein A-I binding protein                          | 1.82  | 1.84   |
| 95356_at    | D00466        | Apolipoprotein e  | 0.71  | 1.20   |
| 101859_at   | AB010100      | Aquaporin 7   | 2.80  | 5.59   |
| 99642_i_at  | X61232        | Carboxypeptidase E  | 0.42  | 0.90   |
| 98543_at    | AJ223208      | Cathepsin S   | 0.47  | 0.77   |
| 98088_at    | X13333        | CD14 antigen  | 0.13  | 0.06   |
| 160358_at   | AI847784      | CD34 antigen  | 0.37  | 0.85   |
| 94939_at    | X97227        | CD53 antigen  | 0.26  | 0.34   |
| 101160_at   | X53798        | Chemokine (C-X-C motif) ligand 2                            | 0.01  | 0.00   |
| 95286_at    | D14077        | Clusterin   | 0.48  | 0.54   |
| 96020_at    | M22531        | Complement component 1, q subcomponent, $\beta$ polypeptide | 0.58  | 0.90   |
| 103353_f_at | D50834        | Cytochrome P-450, subfamily IV B, polypeptide 1             | 1.87  | 3.14   |
| 96912_s_at  | X15591        | Cytotoxic T lymphocyte-associated protein 2 alpha           | 0.42  | 0.68   |
| 94492_at    | AB025406      | Destrin   | 0.44  | 0.63   |
| 104371_at   | AF078752      | Diacylglycerol O-acyltransferase 1                          | 1.80  | 1.39   |
| 92836_at    | AA919594      | Elastin   | 0.60  | 0.70   |
| 94214_at    | X14961        | Fatty acid binding protein 3, muscle and heart              | 2.90  | 4.85   |
| 93459_s_at  | AW122897      | Frizzled homolog 4 (Drosophila)                             | 1.46  | 1.32   |
| 101676_at   | U13705        | Glutathione peroxidase 3                                    | 0.67  | 1.11   |
| 99598_g_at  | AI841629      | Guanine nucleotide binding protein, alpha inhibiting 2      | 0.56  | 0.91   |
| 93277_at    | X53584        | Heat shock protein, 60 kDa                                  | 1.36  | 1.98   |
| 98629_f_at  | Y09085        | Hypoxia inducible factor 1 alpha subunit                    | 0.45  | 0.84   |
| 98773_s_at  | AI323667      | Immunoresponsive gene 1                                     | 0.05  | 0.00   |
| 102658_at   | X59769        | Interleukin 1 receptor, type II                             | 0.23  | 1.21   |
| 99491_at    | U53696        | Interleukin 10 receptor, beta                               | 0.55  | 0.00   |
| 93753_at    | AI852632      | LPS-induced TN factor                                       | 0.56  | 0.56   |
| 94278_at    | D37837        | Lymphocyte cytosolic protein 1                              | 0.42  | 0.29   |
| 99957_at    | X72795        | Matrix metalloproteinase 9                                  | 0.12  | 0.27   |
| 102668_at   | X57638        | Peroxisome proliferator activated receptor alpha            | 1.89  | 2.74   |
| 160481_at   | AF009605      | Phosphoenolpyruvate carboxykinase (pepck) gene co           | 1.56  | 2.23   |
| 104538_at   | AB001607      | Prostaglandin 12 (prostacyclin) synthase                    | 0.44  | 0.65   |
| 101030_at   | X99963        | rhub gene   | 0.54  | 1.07   |
| 103887_at   | M83219        | S100 calcium binding protein A9 (calgranulin B)             | 0.02  | 0.01   |
| 94259_at    | AB024935      | Telomerase binding protein, p23                             | 0.53  | 1.07   |
| 160547_s_at | AI839138      | Thioredoxin interacting protein                             | 2.07  | 2.59   |
| 160532_at   | M22479        | Tropomyosin 1, alpha  | 0.50  | 0.78   |
| 103001_at   | U43836        | Vascular endothelial growth factor B                        | 1.48  | 1.95   |

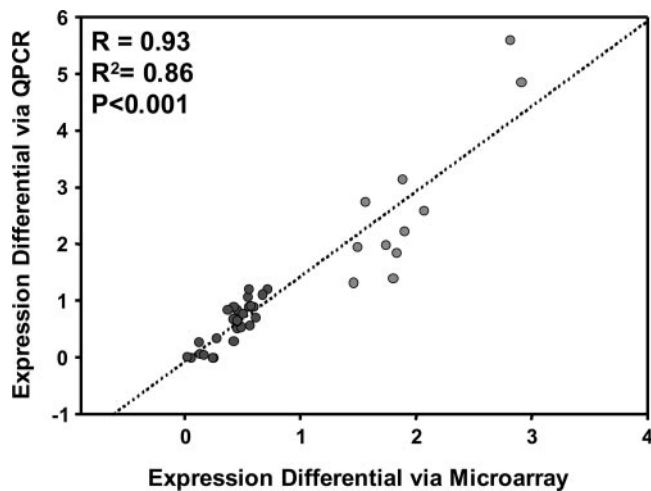


Fig. 2. Correlation between expression differentials (rosiglitazone signal relative to vehicle control) as measured by microarray analysis (x-axis) or by quantitative real-time RT-PCR (y-axis). Light gray and dark gray circles represent up- and downregulated genes, respectively.

2). In an additional study, we examined gene expression levels of these same 39 genes in pooled aortic RNA prepared from independent groups of mice treated with the same protocol as the mice used for the initial microarray analysis. In these samples, there was an agreement of about 70–80% on the up/downregulated calls compared with the initial microarray results (data not shown).

To categorize these genes, each transcript was assigned a function based on the Gene Ontology database and sorted by expression cluster. Cluster analysis (k-means) revealed 3 basic patterns of expression: 29 transcripts of moderate abundance that were decreased (*cluster 0*, –93%) to very low levels, 106 transcripts of high abundance that were downregulated (*cluster 1*, –42%), and 46 transcripts of high abundance that were upregulated (*cluster 2*, +70%). The functional groups with the most significant changes in expression are highlighted in Fig. 3. Transcripts from inflammatory response (–93%,  $n = 6$ ), immune response (–86%,  $n = 7$ ), and cytokine activity

(–82%,  $n = 7$ ) were primarily in *cluster 0*. Those from actin-binding activity (–52%,  $n = 9$ ), calcium-binding activity (–65%,  $n = 10$ ), and cytoskeleton (–46%,  $n = 6$ ) grouped mainly to *cluster 1*. For the oxidoreductase activity group, six transcripts were in *cluster 2* (+72%) and three were present in *cluster 1* (–34%). A list of the individual genes in these functional groups whose expression is changed during rosiglitazone can be found in Table 2.

To gain insight into possible mechanisms by which PPAR $\gamma$  regulates these target genes, we compiled a list of upstream sequences (5 kb) from 142 of the differentially expressed genes. Using a sensitive model to search for PPREs, we detected a total of 117 PPREs in 101 of the sequences examined (Supplemental Table S4). When we examined a similar set of upstream sequences selected randomly from genes not differentially expressed in the microarray experiment, we detected 98 sequences resembling a PPRE in 86 genes. These PPRE-like sequences had more mismatches (3 or more) from consensus compared with the potential PPREs identified from the set of differentially expressed genes, which were a much closer match to the consensus sequence with 50% more (42 vs. 28) having two or fewer mismatches. Comparative sequence analysis was then used to prioritize the search for important regulatory sequences. From the upstream sequences examined, 31 sequence fragments were found to be highly conserved between human and mouse (Table 3). Conserved fragments upstream of basic helix-loop-helix domain containing protein, class B2 (BHLHB2), and frizzled homolog 4 (FZD4) contained a sequence closely resembling a PPRE (Fig. 4). Because PPAR $\gamma$  might also regulate gene transcription by indirect means (activating/inhibiting secondary transcription factors), we looked for the presence of transcription factors among the differentially expressed genes. Of the six transcription factors identified, one was upregulated and five were downregulated (Table 4).

Using genomic location information and orthology between mouse and rat, we mapped 14 of the differentially expressed genes to genomic regions in the rat that have been associated

Fig. 3. Functional groups with the most significant changes in expression during rosiglitazone administration sorted by expression cluster. *Cluster 0* contains 29 transcripts of moderate abundance that were decreased (–93%) to very low levels, *cluster 1* contains 106 transcripts of high abundance that were downregulated (–42%), and *cluster 2* contains 46 transcripts of high abundance that were upregulated (+70%).

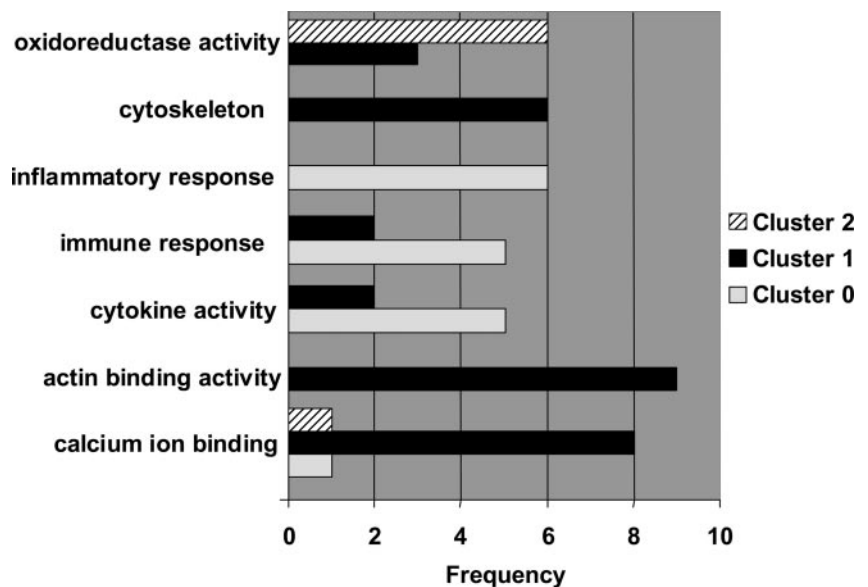


Table 2. *Functional groups identified by cluster analysis*

| Probe Set  | Accession No. | Description   | Change |
|--|---------------|---|--------|
| <i>Actin binding activity (GO:0003779)</i>       |               |   |        |
| 93499_at   | U16740        | Capping protein alpha 1   | 0.80   |
| 93730_at   | AF085809      | Synapsin I  | 0.71   |
| 95142_s_at                                       | U10407        | Capping protein beta 1  | 0.57   |
| 160532_at  | M22479        | Tropomyosin 1, alpha  | 0.50   |
| 94492_at   | AB025406      | Destrin   | 0.45   |
| 160150_f_at                                      | AW125626      | Calponin 3, acidic  | 0.43   |
| 94278_at   | D37837        | Lymphocyte cytosolic protein 1                                    | 0.42   |
| 97384_at   | AA791012      | Glia maturation factor, gamma                                     | 0.36   |
| 97990_at   | D85923        | Myosin heavy chain 11, smooth muscle                              | 0.34   |
| <i>Calcium ion binding activity (GO:0005509)</i> |               |   |        |
| 99536_at   | AB016080      | Kinase interacting protein 2                                      | 1.76   |
| 98600_at   | U41341        | S100 calcium binding protein A11 (calizzarin)                     | 0.66   |
| 103721_at  | AA592182      | Nephronectin  | 0.49   |
| 92770_at   | X66449        | S100 calcium binding protein A6 (calcyclin)                       | 0.48   |
| 94278_at   | D37837        | Lymphocyte cytosolic protein 1                                    | 0.42   |
| 101393_at  | AJ001633      | Annexin A3  | 0.40   |
| 93281_at   | AF049125      | Reticulocalbin 2  | 0.40   |
| 93866_s_at                                       | D00613        | Matrix gamma-carboxyglutamate (gla) protein                       | 0.40   |
| 161703_f_at                                      | AV003419      | Annexin A1  | 0.38   |
| 103887_at  | M83219        | S100 calcium binding protein A9 (calgranulin B)                   | 0.02   |
| <i>Cytokine activity (GO:0005125)</i>            |               |   |        |
| 98600_at   | U41341        | S100 calcium binding protein A11 (calizzarin)                     | 0.66   |
| 104388_at  | U49513        | Chemokine (C-C motif) ligand 9                                    | 0.38   |
| 95348_at   | J04596        | Chemokine (C-X-C motif) ligand 1                                  | 0.25   |
| 102424_at  | J04491        | Chemokine (C-C motif) ligand 3                                    | 0.06   |
| 97519_at   | X13986        | Secreted phosphoprotein 1   | 0.02   |
| 101160_at  | X53798        | Chemokine (C-X-C motif) ligand 2                                  | 0.01   |
| 103486_at  | M15131        | Interleukin 1 beta  | 0.01   |
| <i>Cytoskeleton (GO:0005200)</i>                 |               |   |        |
| 93499_at   | U16740        | Capping protein alpha 1   | 0.80   |
| 101578_f_at                                      | M12481        | Actin, beta, cytoplasmic  | 0.58   |
| 95142_s_at                                       | U10407        | Capping protein beta 1  | 0.57   |
| 96573_at   | M21495        | Actin, gamma, cytoplasmic   | 0.55   |
| 160532_at  | M22479        | Tropomyosin 1, alpha  | 0.50   |
| 93100_at   | X13297        | Actin, alpha 2, smooth muscle, aorta                              | 0.45   |
| <i>Immune response (GO:0006955)</i>              |               |   |        |
| 101054_at  | X00496        | Ia-associated invariant chain                                     | 0.61   |
| 104388_at  | U49513        | Chemokine (C-C motif) ligand 9                                    | 0.38   |
| 95348_at   | J04596        | Chemokine (C-X-C motif) ligand 1                                  | 0.25   |
| 98088_at   | X13333        | CD14 antigen  | 0.13   |
| 102424_at  | J04491        | Chemokine (C-C motif) ligand 3                                    | 0.06   |
| 101160_at  | X53798        | Chemokine (C-X-C motif) ligand 2                                  | 0.01   |
| 103486_at  | M15131        | Interleukin 1 beta  | 0.01   |
| <i>Inflammatory response (GO:0006954)</i>        |               |   |        |
| 95348_at   | J04596        | Chemokine (C-X-C motif) ligand 1                                  | 0.25   |
| 98988_at   | AA614971      | Molecule possessing ankyrin-repeats induced by lipopolysaccharide | 0.20   |
| 98088_at   | X13333        | CD14 antigen  | 0.13   |
| 102424_at  | J04491        | Chemokine (C-C motif) ligand 3                                    | 0.06   |
| 101160_at  | X53798        | Chemokine (C-X-C motif) ligand 2                                  | 0.01   |
| 103486_at  | M15131        | Interleukin 1 beta  | 0.01   |
| <i>Oxidoreductase activity (GO:0016491)</i>      |               |   |        |
| 93844_at   | AW061302      | RIKEN cDNA 1100001F06 gene  | 1.94   |
| 103353_f_at                                      | D50834        | Cytochrome P-450, subfamily IV B, polypeptide 1                   | 1.88   |
| 95693_at   | U51167        | Isocitrate dehydrogenase 2 (NADP <sup>+</sup> ), mitochondrial    | 1.54   |
| 101525_at  | AI848871      | RIKEN cDNA 0610011B04 gene  | 1.47   |
| 95053_s_at                                       | AA674669      | RIKEN cDNA 0710008N11 gene  | 1.46   |
| 96899_at   | AW123802      | NADH dehydrogenase (ubiquinone) Fe-S protein 3                    | 1.38   |
| 101676_at  | U13705        | Glutathione peroxidase 3  | 0.67   |
| 100068_at  | M74570        | Aldehyde dehydrogenase family 1, subfamily A1                     | 0.61   |
| 97013_f_at                                       | AW046124      | Cytochrome b-245, alpha polypeptide                               | 0.51   |

Table 3. Conserved sequences between human and mouse in 5' flanking region of differentially expressed genes

| Accession No. | Description  | Location  | Start Sequence | PPRE |
|---------------|--|-----------|----------------|------|
| X13297        | Actin, alpha 2, smooth muscle, aorta               | 333-1     | GCTGGCATCTTC   | N    |
| M12481        | Actin, beta, cytoplasmic                           | 135-7     | TGCTGCACTGTG   | N    |
| U19118        | Activating transcription factor 3                  | 315-155   | CAACCTAGCGGA   | N    |
| D00466        | Apolipoprotein e                                   | 3901-3791 | CCAGCTGCAGGT   | N    |
| Y07836        | Basic helix-loop-helix domain containing, class B2 | 1833-1676 | CAGCCAGGTCAC   | 1739 |
| Y07836        | Basic helix-loop-helix domain containing, class B2 | 999-834   | GGCCACGTGAAG   | N    |
| D14077        | Clusterin  | 121-3     | CCCCACCTCTA    | N    |
| AW047343      | D site albumin promoter binding protein            | 1955-1791 | CGCAGATGATGC   | N    |
| AW047343      | D site albumin promoter binding protein            | 1700-1526 | GCAGATGCACTC   | N    |
| V00727        | fbj osteosarcoma oncogene                          | 528-412   | CTGCACCCCTCAG  | N    |
| V00727        | fbj osteosarcoma oncogene                          | 2086-1923 | GCCTAAATTCCTC  | N    |
| V00727        | fbj osteosarcoma oncogene                          | 1894-1657 | TCAGCCCCCGGA   | N    |
| AW122897      | frizzled homolog 4 ( <i>Drosophila</i> )           | 3572-3296 | TAATAATGAATC   | N    |
| AW122897      | frizzled homolog 4 ( <i>Drosophila</i> )           | 899-693   | TTGTGCGCCTTC   | 878  |
| U57524        | i kappa b alpha gene exons 2-6 partial cds         | 499-135   | AAGCGAATCCCT   | N    |
| U57524        | i kappa b alpha gene exons 2-6 partial cds         | 129-13    | GAGGACGAGCCA   | N    |
| U69543        | Lipase hormone sensitive                           | 4850-4744 | TTTATTTGTGCC   | N    |
| M69260        | Lipocortin 1                                       | 147-20    | GAGTAGTTTTGC   | N    |
| AW123802      | NADH dehydrogenase (ubiquinone) Fe-S protein 3     | 1595-844  | CTTACTGAGAT    | N    |
| AW125185      | Open reading frame 18                              | 1155-983  | CAGTCCTGTGCA   | N    |
| Z38110        | Peripheral myelin protein, 22 kDa                  | 2686-2541 | CCTGCAAGGCCT   | N    |
| X52046        | Procollagen type iii alpha 1                       | 275-111   | CTCCAGATGTGC   | N    |
| X58251        | Procollagen, type I, alpha 2                       | 247-0     | CCGGGGCCCTA    | N    |
| X58251        | Procollagen, type I, alpha 2                       | 2598-2486 | CCACCAAGTGCT   | N    |
| X58251        | Procollagen, type I, alpha 2                       | 465-316   | GTGTCTCTAAAGT  | N    |
| X99963        | rhob gene  | 563-362   | GCCTCTCCAGC    | N    |
| A1853864      | RIKEN cDNA 2010100O12 gene                         | 4503-4384 | TCCCTCCTCCTA   | N    |
| M83219        | S100 calcium binding protein A9 (calgranulin B)    | 202-63    | AACCAGTTTCCC   | N    |
| U88567        | Secreted frizzled-related sequence protein 2       | 187-5     | GGGTGGGGGCG    | N    |
| AI840996      | Selenoprotein R                                    | 964-833   | CCCAGTCCCTTC   | N    |
| M22479        | Tropomyosin 1, alpha                               | 285-62    | TCCAGGGGTGC    | N    |

PPRE, PPAR response element.

with increased blood pressure (Table 5). We also examined whether groups of differentially expressed genes are closely linked to a blood pressure QTL (1 Mb). Several members of a small inducible cytokine family [known as CCL or chemokine (C-C motif) ligand] are located in a 400-kb stretch on mouse chromosome 11. This region is syntenic to a region on rat chromosome 10 containing a blood pressure QTL. As expected, the rat ortholog of mouse CCL3 has been mapped to this region. CCL3 (accession no. J04491) was decreased by rosiglitazone. Another member of the family, CCL9 (accession no. U49513) was also decreased by rosiglitazone; however, the rat ortholog of mouse CCL9 has not been conclusively determined at this time.

In the present study, RNA was prepared from the whole aorta, making it difficult to discern the contribution of each of the vascular cell types to the overall gene expression profile. In particular, it would be attractive if existing publicly available resources could be integrated with our data to ascertain the cell expression pattern of the differentially expressed genes. The Cancer Genome Anatomy Project at the National Institutes of Health has compiled serial analysis of gene expression (SAGE) results from several different tissue/cell types under both control and experimental/diseased conditions. The only available library derived from cells present in the vessel wall was from human microvascular endothelial cells (Library ID: 29). We combined the information from this library with our complete list of differentially expressed genes (Supplemental Tables S2 and S3) to generate a subset of genes that are likely to be highly expressed in endothelial cells (Table 6).

## DISCUSSION

The major finding of the present study is that chronic treatment with a PPAR $\gamma$  agonist is associated with significant changes in a number of biologically important pathways in mouse aorta. A significant correlation was observed between the microarray results and real-time RT-PCR analysis of 39 of these genes, suggesting that oligonucleotide array-based assays of gene expression are a reliable way to interrogate gene expression of a large number of genes in an unbiased manner.

The actions of the TZDs, including rosiglitazone, are believed to be mediated primarily by activation of PPAR $\gamma$ , although results from some studies suggest that a contribution from PPAR $\alpha$  activation or from a non-PPAR-related mechanism might exist as well (3). We recognize that the dose of rosiglitazone used herein is similar to that which has been reported in the literature for animal studies but is higher than the standard dose used in the treatment of non-insulin-dependent diabetes mellitus. Therefore, we cannot definitely rule out the possibility that some of the changes in gene expression may be due to this. This dose was effective in lowering blood pressure and improving vascular function in a hypertensive mouse model (24). Indeed, in some experimental hypertensive models, PPAR $\gamma$  agonists significantly lower blood pressure, and it has been proposed that this action is responsible for at least part of the vascular protective actions of PPAR $\gamma$  (7). Although we did not measure blood pressure in the mice used in the microarray experiment, we did not observe any change in blood pressure in previous studies of normal control mice administered rosiglitazone at the same dose used herein (24).

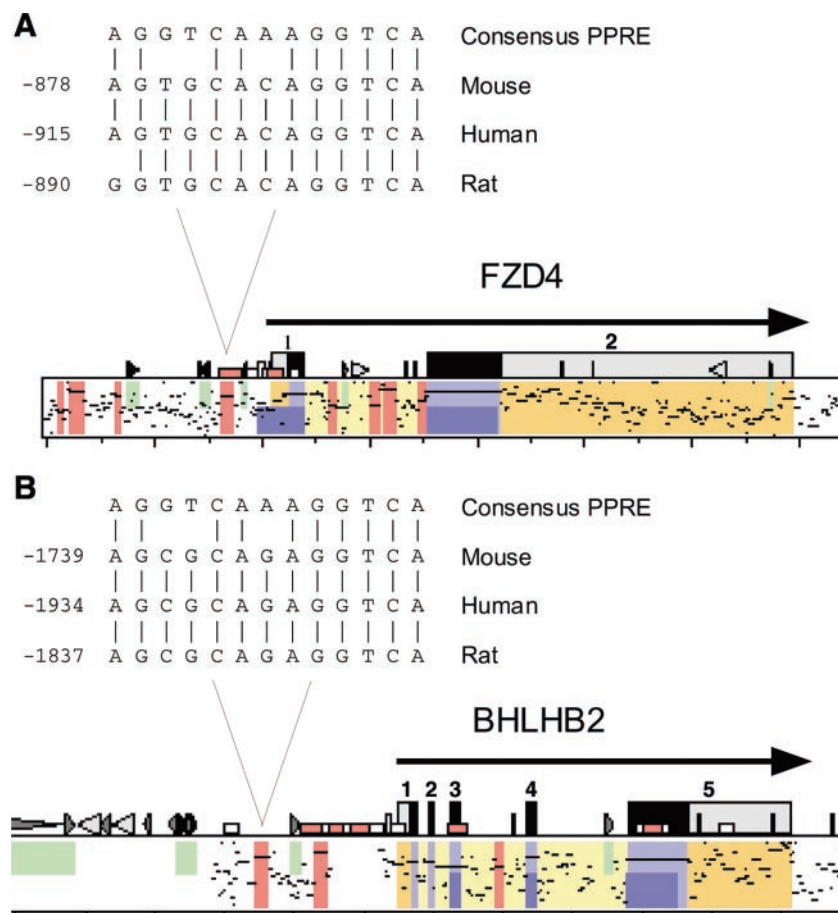


Fig. 4. Percent identity plots showing potential PPAR response elements (PPREs) upstream of two genes differentially expressed during rosiglitazone administration. Both of these potential PPREs are located in regions of highly conserved noncoding sequence (indicated by the red color). A: frizzled homolog 4 (FZD4). B: basic helix-loop-helix containing protein, class B2 (BHLHB2).

*PPAR $\gamma$  in blood vessel wall.* PPAR $\gamma$  is expressed in vascular smooth muscle (13), vascular endothelium (5), and macrophages (22), and the mechanisms responsible for the known actions of PPAR $\gamma$  in the vasculature appear to involve functional changes in each of these cell types. In cultured vascular smooth muscle cells, PPAR $\gamma$  has actions similar to that observed in animal models. That is, it inhibits cell migration and attenuates the induction of matrix metalloproteinases (MMPs), a key step in cell invasion (16). The finding of a significant decrease in MMP-9 mRNA in aorta from rosiglitazone-treated mice in the present study is consistent with those results. Recent evidence suggests that downregulation of the type 1 receptor for angiotensin II in the vascular smooth muscle cell may play a role in the blood pressure lowering and vascular protective actions of PPAR $\gamma$  (26). However, in the present study we did not detect any changes in expression of components of the renin-angiotensin system, all of which were on the array.

Alterations in endothelial cell function may contribute to the vascular actions of PPAR $\gamma$ . PPAR $\gamma$  may protect the endothelium against high levels of reactive oxygen species such as superoxide by increasing expression of scavenger enzymes including Cu-superoxide dismutase (11) and catalase (8) and by decreasing expression of the p22 and p47 phox subunits of the superoxide-generating enzyme NADPH oxidase (11). In the present study, we identified in mouse aorta nine differentially expressed genes involved in oxidative-reduction reactions. The functional contribution of these pathways to the chronic regulation of vascular tone remains to be elucidated. PPAR $\gamma$  has several other endothelial-specific actions, including decreased secretion of endothelin (5), a potent vasoconstrictor, and reduced expression of adhesion molecules on the endothelial cell surface (7), a key step in the atherogenic process. In our rosiglitazone-treated mice, there were no significant changes in endothelin or in any of the nitric oxide synthase isoforms. There was, in contrast, a marked decrease in

Table 4. Differentially regulated transcription factors

| Probe Set   | Accession No. | Description  | Change |
|-------------|---------------|--|--------|
| 102668_at   | X57638        | Peroxisome proliferator activated receptor alpha   | 1.90   |
| 104155_f_at | U19118        | Activating transcription factor 3                  | 0.46   |
| 98628_f_at  | AF003695      | Hypoxia inducible factor 1, alpha subunit          | 0.44   |
| 160841_at   | AW047343      | D site albumin promoter binding protein            | 0.32   |
| 98988_at    | AA614971      | Molecule possessing ankyrin-repeats induced by LPS | 0.20   |
| 104701_at   | Y07836        | Basic helix-loop-helix domain containing, class B2 | 0.16   |

Table 5. *Differentially expressed genes in blood pressure QTLs*

| Probe Set   | Accession No. | Description                                     | Mouse Chr | Rat Chr | Change |
|-------------|---------------|---|-----------|---------|--------|
| 161689_f_at | AV223216      | Interleukin 1 receptor, type II                 | 1         | 9       | 0.13   |
| 102658_at   | X59769        | Interleukin 1 receptor, type II                 | 1         | 9       | 0.24   |
| 98451_at    | AI843164      | DnaJ (Hsp40) homolog, subfamily B, member 10    | 1         | 9       | 0.58   |
| 93277_at    | X53584        | Heat shock protein, 60 kDa                      | 1         | 9       | 1.36   |
| 100566_at   | L12447        | Insulin-like growth factor binding protein 5    | 1         | 9       | 0.42   |
| 95477_at    | AW125185      | Open reading frame 18                           | 4         | 5       | 0.63   |
| 103353_f_at | D50834        | Cytochrome P-450, subfamily IV B, polypeptide 1 | 4         | 5       | 1.88   |
| 100437_g_at | M27008        | Orosomucoid 1                                   | 4         | 5       | 0.85   |
| 95787_s_at  | X87685        | Sterol carrier protein 2-pseudogene             | 4         | 5       | 1.55   |
| 160108_at   | AI852641      | Nuclear protein 1                               | 7         | 1       | 0.65   |
| 102395_at   | Z38110        | Peripheral myelin protein, 22kDa                | 11        | 10      | 0.63   |
| 94469_at    | AW120950      | Expressed sequence AI182287                     | 11        | 10      | 0.63   |
| 92471_i_at  | AF099973      | Schlafen 2                                      | 11        | 10      | 0.28   |
| 102424_at   | J04491        | Chemokine (C-C motif) ligand 3                  | 11        | 10      | 0.06   |
| 101054_at   | X00496        | Ia-associated invariant chain                   | 18        | 18      | 0.61   |

expression of several adhesion molecules, a finding consistent with previous reports (7).

One of the first steps in vascular lesion formation is the attachment of circulating monocytes to the endothelium of the vascular wall followed by the release of proinflammatory mediators from activated macrophages. Recent studies with animal models of atherosclerosis have demonstrated that TZDs reduce the number and size of lesions formed in the vascular wall, in part, by attenuating the inflammatory responses of infiltrating macrophages (4). PPAR $\gamma$  agonists have recently been shown to have anti-inflammatory actions in other disease conditions including inflammatory bowel disease (1) and al-

lergic encephalomyelitis (6), suggesting that this action is not vascular specific. Moreover, these responses to PPAR $\gamma$  agonists may not require the presence of atherosclerosis or a severe inflammatory condition. For example, in the present study, under basal conditions in which expression of inflammatory mediators would be expected to be relatively low, rosiglitazone treatment was associated with almost complete repression of several genes involved in the inflammatory response.

*Genomic approaches to complex pathways.* Sequence-based approaches can be used to gain insight into possible mechanisms by which PPAR $\gamma$  regulates the target genes identified in this study. To do this, we compiled a list of upstream sequences

Table 6. *Differentially expressed genes in endothelial SAGE library*

| Probe Set   | Accession No. | Description  | Mouse Unigene | Human Unigene | Change |
|-------------|---------------|--|---------------|---------------|--------|
| 160547_s_at | AI839138      | Thioredoxin interacting protein                                | Mm.77432      | Hs.179526     | 2.07   |
| 95690_at    | AW047363      | RIKEN cDNA 1110030L07 gene                                     | Mm.29651      | Hs.4877       | 2.03   |
| 104164_at   | AI181257      | RIKEN cDNA 1300019N10 gene                                     | Mm.27139      | Hs.15386      | 1.92   |
| 160558_at   | U22445        | Thymoma viral proto-oncogene 2                                 | Mm.177194     | Hs.326445     | 1.81   |
| 93780_at    | AW060827      | RIKEN cDNA 0610006O17 gene                                     | Mm.2125       | Hs.9676       | 1.80   |
| 160904_at   | AI841484      | Hypothetical protein, clone 1-82                               | Mm.5166       | Hs.351871     | 1.79   |
| 97422_at    | AW048882      | <i>Mus musculus</i> , clone IMAGE:3982770, mRNA, partial cds   | Mm.29999      | Hs.197289     | 1.74   |
| 95736_at    | AI847546      | Mitochondrial ribosomal protein L4                             | Mm.155033     | Hs.279652     | 1.68   |
| 95693_at    | U51167        | Isocitrate dehydrogenase 2 (NADP <sup>+</sup> ), mitochondrial | Mm.2966       | Hs.429        | 1.54   |
| 96348_at    | AW121217      | RIKEN cDNA 0610039C21 gene                                     | Mm.29998      | Hs.118463     | 1.52   |
| 103001_at   | U43836        | Vascular endothelial growth factor B                           | Mm.15607      | Hs.78781      | 1.49   |
| 95053_s_at  | AA674669      | RIKEN cDNA 0710008N11 gene                                     | Mm.29141      | Hs.64         | 1.46   |
| 97880_at    | AW061024      | RIKEN cDNA 4930529O08 gene                                     | Mm.28365      | Hs.296348     | 1.40   |
| 96899_at    | AW123802      | NADH dehydrogenase (ubiquinone) Fe-S protein 3                 | Mm.30113      | Hs.429506     | 1.38   |
| 104598_at   | X61940        | Dual specificity phosphatase 1                                 | Mm.2404       | Hs.171695     | 0.66   |
| 98600_at    | U41341        | S100 calcium binding protein A11 (calizzarin)                  | Mm.175848     | Hs.417004     | 0.66   |
| 93593_f_at  | U87948        | Epithelial membrane protein 3                                  | Mm.20829      | Hs.9999       | 0.64   |
| 94469_at    | AW120950      | Expressed sequence AI182287                                    | Mm.28848      | Hs.54642      | 0.63   |
| 96657_at    | L10244        | Spermidine/spermine N1-acetyl transferase                      | Mm.2734       | Hs.28491      | 0.62   |
| 95542_at    | AI835858      | ESTs, Moderately similar to S11390 tropomyosin 5 - mouse       | Mm.27685      | Hs.250641     | 0.57   |
| 97013_f_at  | AW046124      | Cytochrome b-245, alpha polypeptide                            | Mm.448        | Hs.68877      | 0.51   |
| 96146_at    | D83745        | B-cell translocation gene 3                                    | Mm.2823       | Hs.77311      | 0.46   |
| 100088_at   | M27073        | Protein phosphatase 1, catalytic subunit, beta isoform         | Mm.4572       | Hs.21537      | 0.43   |
| 99642_i_at  | X61232        | Carboxypeptidase E   | Mm.31395      | Hs.75360      | 0.42   |
| 94061_at    | M13018        | Cysteine rich intestinal protein                               | Mm.22049      | Hs.423190     | 0.42   |
| 100566_at   | L12447        | Insulin-like growth factor binding protein 5                   | Mm.578        | Hs.380833     | 0.42   |
| 93281_at    | AF049125      | Reticulocalbin 2   | Mm.1782       | Hs.79088      | 0.40   |
| 160358_at   | AI847784      | CD34 antigen   | Mm.29798      | Hs.374990     | 0.37   |
| 97384_at    | AA791012      | Glia maturation factor, gamma                                  | Mm.29766      | Hs.5210       | 0.36   |
| 102779_at   | X54149        | Growth arrest and DNA-damage-inducible 45 beta                 | Mm.1360       | Hs.110571     | 0.26   |
| 161666_f_at | AV138783      | Growth arrest and DNA-damage-inducible 45 beta                 | Mm.1360       | Hs.110571     | 0.05   |
| 97519_at    | X13986        | Secreted phosphoprotein 1                                      | Mm.321        | Hs.313        | 0.02   |

(5 kb) from 142 of the differentially expressed genes. Using a sensitive model to search for PPREs, we were unable to detect PPREs in about 30% of the sequences examined. The fact that not all of the regions examined contained a binding sequence for PPAR $\gamma$  might suggest either that the response element is located outside of the sequence analyzed or that these genes are indirectly regulated by PPAR $\gamma$ . The presence of six transcription factors among the differentially expressed genes provides support for the idea that PPAR $\gamma$  regulates target gene transcription via indirect (activating/inhibiting secondary transcription factors) and direct (binding to PPREs) mechanisms.

Comparative sequence analysis has been used to prioritize the genomic region in which to search for important regulatory sequences. Those locations in the genome most highly conserved between different species are likely to be enriched in biologically important sequences (28). Using this approach, previously unknown regulatory elements for the stem cell leukemia gene and for several genes important in the inflammatory response were discovered (9, 15). From the upstream sequences examined in this study, 31 sequence fragments were found to be highly conserved between human and mouse, and 2 of these contained a sequence closely resembling a PPRE. Of course, this does not rule out the functional importance of the other 99 PPRE sequences.

The two conserved PPREs are located upstream of BHLHB2 and FZD4. There are no published reports of a linkage between FZD4 and PPAR $\gamma$ , although several recent studies in human patients have provided evidence that lack of FZD4, a member of the Wnt-signaling pathway, impairs normal retinal vascularization (23). BHLHB2, a transcription factor, appears to be an important downstream mediator of hypoxia-induced changes in gene expression and inhibits expression of the PPAR $\gamma$  gene in adipocytes (30). During chronic rosiglitazone treatment, we observed significant decreases in expression of hypoxia inducible factor 1 (−56%) and in BHLHB2 (−84%). There was a tendency for decreased expression of PPAR $\gamma$  (−29%) that was not statistically significant. These findings suggest the possibility that a negative feedback relationship between PPAR $\gamma$  and hypoxia-induced genes may exist in the vasculature, although future studies are required to test this hypothesis.

*PPAR $\gamma$ , blood vessel wall, and hypertension.* In several disease conditions including atherosclerosis and hypertension, relatively large genomic regions associated with a particular disease trait (QTL regions) have been defined. However, because these chromosomal regions are large, elucidation of the exact genetic variations responsible for these associations has been difficult. In a recent report, microarray data and computational methods were combined to prioritize the list of candidate genes for human cytochrome *c* oxidase deficiency, and the causative gene was discovered (19). Given the established importance of the PPAR $\gamma$  pathway in vascular function and blood pressure, the 14 differentially expressed genes from the present study that map to rat blood pressure QTL regions should be considered as potential candidate genes for further study.

Thus chronic administration of a PPAR $\gamma$  agonist elicits changes in numerous genetic pathways in mouse aorta. By combining large-scale gene expression analysis with oligonucleotide microarrays and bioinformatic approaches, we were able to identify, in a nonbiased manner, 181 differentially

expressed genes, 14 of which map to rat blood pressure QTL regions. Further studies are required to determine the functional consequence of over/underexpression of these genes, to evaluate the importance of genomic DNA sequences upstream of these genes predicted to contain important regulatory domains, and to dissect the contribution of the various vascular cell types to the integrated response.

#### ACKNOWLEDGMENTS

We thank Deborah R. Davis for assistance with the mice used in this study. S. R. Gullans served as the review editor for this manuscript submitted by Editor C. D. Sigmund.

#### GRANTS

This work was supported by National Institutes of Health Grants HL-48058, HL-61446, HL-55006 (to C. D. Sigmund) and the Center for Bioinformatics and Computational Biology at the University of Iowa. We gratefully acknowledge the generous research support of the Roy J. Carver Trust.

#### REFERENCES

1. **Auwerx J.** Nuclear receptors. I. PPAR $\gamma$  in the gastrointestinal tract: gain or pain? *Am J Physiol Gastrointest Liver Physiol* 282: G581–G585, 2002; 10.1152/ajpgi.00508.2001.
2. **Barroso I, Gurnell M, Crowley VE, Agostini M, Schwabe JW, Soos MA, Maslen GL, Williams TD, Lewis H, Schafer AJ, Chatterjee VK, and O'Rahilly S.** Dominant negative mutations in human PPAR $\gamma$  associated with severe insulin resistance, diabetes mellitus and hypertension. *Nature* 402: 880–883, 1999.
3. **Berger J and Moller DE.** The mechanisms of action of PPARs. *Annu Rev Med* 53: 409–435, 2002.
4. **Chen Z, Ishibashi S, Perrey S, Osuga J, Gotoda T, Kitamine T, Tamura Y, Okazaki H, Yahagi N, Iizuka Y, Shionoiri F, Ohashi K, Harada K, Shimano H, Nagai R, and Yamada N.** Troglitazone inhibits atherosclerosis in apolipoprotein E-knockout mice: pleiotropic effects on CD36 expression and HDL. *Arterioscler Thromb Vasc Biol* 21: 372–377, 2001.
5. **Deliver P, Martin-Nizard F, Chinetti G, Trottein F, Fruchart JC, Najib J, Duriez P, and Staels B.** Peroxisome proliferator-activated receptor activators inhibit thrombin-induced endothelin-1 production in human vascular endothelial cells by inhibiting the activator protein-1 signaling pathway. *Circ Res* 85: 394–402, 1999.
6. **Diab A, Deng C, Smith JD, Hussain RZ, Phanavanh B, Lovett-Racke AE, Drew PD, and Racke MK.** Peroxisome proliferator-activated receptor-gamma agonist 15-deoxy-Delta(12,14)-prostaglandin J(2) ameliorates experimental autoimmune encephalomyelitis. *J Immunol* 168: 2508–2515, 2002.
7. **Diep QN, El Mabrouk M, Cohn JS, Endemann D, Amiri F, Viridis A, Neves MF, and Schiffrin EL.** Structure, endothelial function, cell growth, and inflammation in blood vessels of angiotensin II-infused rats: role of peroxisome proliferator-activated receptor-gamma. *Circulation* 105: 2296–2302, 2002.
8. **Girnun GD, Domann FE, Moore SA, and Robbins ME.** Identification of a functional peroxisome proliferator-activated receptor response element in the rat catalase promoter. *Mol Endocrinol* 16: 2793–2801, 2002.
9. **Gottgens B, Barton LM, Chapman MA, Sinclair AM, Knudsen B, Grafham D, Gilbert JG, Rogers J, Bentley DR, and Green AR.** Transcriptional regulation of the stem cell leukemia gene (SCL): comparative analysis of five vertebrate SCL loci. *Genome Res* 12: 749–59, 2002.
10. **Haverty PM, Hansen U, and Weng Z.** Computational inference of transcriptional regulatory networks from expression profiling and transcription factor binding site identification. *Nucleic Acids Res* 32: 179–188, 2004.
11. **Inoue I, Goto S, Matsunaga T, Nakajima T, Awata T, Hokari S, Komoda T, and Katayama S.** The ligands/activators for peroxisome proliferator-activated receptor alpha (PPARalpha) and PPARgamma increase Cu<sup>2+</sup>, Zn<sup>2+</sup>-superoxide dismutase and decrease p22phox message expressions in primary endothelial cells. *Metabolism* 50: 3–11, 2001.
12. **Kasprzyk A, Keefe D, Smedley D, London D, Spooner W, Melsopp C, Hammond M, Rocca-Serra P, Cox T, and Birney E.** Ensembl: a generic system for fast and flexible access to biological data. *Genome Res* 14: 160–169, 2004.

13. Law RE, Goetze S, Xi XP, Jackson S, Kawano Y, Demer L, Fishbein MC, Meehan WP, and Hsueh WA. Expression and function of PPAR-gamma in rat and human vascular smooth muscle cells. *Circulation* 101: 1311–1318, 2000.
14. Law RE, Meehan WP, Xi XP, Graf K, Wuthrich DA, Coats W, Faxon D, and Hsueh WA. Troglitazone inhibits vascular smooth muscle cell growth and intimal hyperplasia. *J Clin Invest* 98: 1897–1905, 1996.
15. Loots GG, Locksley RM, Blankespoor CM, Wang ZE, Miller W, Rubin EM, and Frazer KA. Identification of a coordinate regulator of interleukins 4, 13, and 5 by cross-species sequence comparisons. *Science* 288: 136–140, 2000.
16. Marx N, Schonbeck U, Lazar MA, Libby P, and Plutzky J. Peroxisome proliferator-activated receptor gamma activators inhibit gene expression and migration in human vascular smooth muscle cells. *Circ Res* 83: 1097–1103, 1998.
17. Mayerson AB, Hundal RS, Dufour S, Lebon V, Befroy D, Cline GW, Enocksson S, Inzucchi SE, Shulman GI, and Petersen KF. The effects of rosiglitazone on insulin sensitivity, lipolysis, and hepatic and skeletal muscle triglyceride content in patients with type 2 diabetes. *Diabetes* 51: 797–802, 2002.
18. Miyazaki Y, Mahankali A, Matsuda M, Glass L, Mahankali S, Ferrannini E, Cusi K, Mandarino LJ, and DeFronzo RA. Improved glycemic control and enhanced insulin sensitivity in type 2 diabetic subjects treated with pioglitazone. *Diabetes Care* 24: 710–719, 2001.
19. Mootha VK, Lepage P, Miller K, Bunkenborg J, Reich M, Hjerrild M, Delmonte T, Villeneuve A, Sladek R, Xu F, Mitchell GA, Morin C, Mann M, Hudson TJ, Robinson B, Rioux JD, and Lander ES. Identification of a gene causing human cytochrome c oxidase deficiency by integrative genomics. *Proc Natl Acad Sci USA* 100: 605–610, 2003.
20. Mueller E, Drori S, Aiyer A, Yie J, Sarraf P, Chen H, Hauser S, Rosen ED, Ge K, Roeder RG, and Spiegelman BM. Genetic analysis of adipogenesis through peroxisome proliferator-activated receptor gamma isoforms. *J Biol Chem* 277: 41925–41930, 2002.
21. Ogihara T, Rakugi H, Ikegami H, Mikami H, and Masuo K. Enhancement of insulin sensitivity by troglitazone lowers blood pressure in diabetic hypertensives. *Am J Hypertens* 8: 316–320, 1995.
22. Ricote M, Li AC, Willson TM, Kelly CJ, and Glass CK. The peroxisome proliferator-activated receptor-gamma is a negative regulator of macrophage activation. *Nature* 391: 79–82, 1998.
23. Robitaille J, MacDonald ML, Kaykas A, Sheldahl LC, Zeisler J, Dube MP, Zhang LH, Singaraja RR, Guernsey DL, Zheng B, Siebert LF, Hoskin-Mott A, Trese MT, Pimstone SN, Shastry BS, Moon RT, Hayden MR, Goldberg YP, and Samuels ME. Mutant frizzled-4 disrupts retinal angiogenesis in familial exudative vitreoretinopathy. *Nat Genet* 32: 326–330, 2002.
24. Ryan MJ, Didion SP, Mathur S, Faraci FM, and Sigmund CD. PPAR $\gamma$  agonist rosiglitazone improves vascular function and lowers blood pressure in hypertensive transgenic mice. *Hypertension* 43: 661–666, 2004.
25. Sandelin A, Alkema W, Engstrom P, Wasserman WW, and Lenhard B. JASPAR: an open-access database for eukaryotic transcription factor binding profiles. *Nucleic Acids Res* 32: D91–D94, 2004.
26. Takeda K, Ichiki T, Tokunou T, Funakoshi Y, Iino N, Hirano K, Kanaide H, and Takeshita A. Peroxisome proliferator-activated receptor gamma activators downregulate angiotensin II type 1 receptor in vascular smooth muscle cells. *Circulation* 102: 1834–1839, 2000.
27. Walker AB, Dores J, Buckingham RE, Savage MW, and Williams G. Impaired insulin-induced attenuation of noradrenaline-mediated vasoconstriction in insulin-resistant obese Zucker rats. *Clin Sci (Lond)* 93: 235–241, 1997.
28. Wasserman WW, Palumbo M, Thompson W, Fickett JW, and Lawrence CE. Human-mouse genome comparisons to locate regulatory sites. *Nat Genet* 26: 225–228, 2000.
29. Watanabe Y, Sunayama S, Shimada K, Sawano M, Hoshi S, Iwama Y, Mokuno H, Daida H, and Yamaguchi H. Troglitazone improves endothelial dysfunction in patients with insulin resistance. *J Atheroscler Thromb* 7: 159–163, 2000.
30. Yun Z, Maecker HL, Johnson RS, and Giaccia AJ. Inhibition of PPAR gamma 2 gene expression by the HIF-1-regulated gene DEC1/Stra13: a mechanism for regulation of adipogenesis by hypoxia. *Dev Cell* 2: 331–341, 2002.

